Functional organization of social perception in the human brain

Supplementary materials

Supplementary methods

Hierarchical clustering of social features

Unweighted pair group method with arithmetic mean (UPGMA), as implemented in R, was used as the clustering algorithm (https://www.rdocumentation.org/packages/stats/versions/3.6.2/topics/hclust). Other average linkage clustering methods implemented in the R package (WPGMA, WPGMC and UPGMC) yielded highly similar clustering hierarchy. Hierarchical clustering requires a desired number of resulting clusters as an input for automatic definition of cluster boundaries from hierarchical tree (**Figure SI-2**). To estimate the optimal number of clusters we chose three criteria that the clustering result should satisfy. These were cluster stability, theoretically meaningful clustering, and sufficient reduction in collinearity between the clusters. To assess the stability of clusters with different number of clusters we conducted a consensus clustering analysis with ConsensusClusterPlus R package (Wilkerson & Hayes, 2010). In consensus clustering analysis 80% of stimulus time points and 80% of social features were randomly sampled and then clustered using UPGMA. Data were resampled 5000 times and then the stability of clusters with different number of clusters (k) was assessed based on the consensus of the resampling (**Figure SI-3**). Analysis showed that clustering results stabilize when $k > 10$ (Relative change in area under curve between CDFs of the consensus matrix of k clusters and k - 1 clusters is minimal, **Figure SI-3 a & b**). In addition, $k = 13$ was the lowest number of clusters yielding in theoretically meaningful cluster labels. With 13 clusters, maximum pairwise correlation between any two resulting regressors of the model was below 0.4 and maximum VIF value was 3.3 (male regressor) which was considered as sufficient reduction in collinearity.

Ridge regression

Ridge regression uses L2-regularization where OLS β-coefficient estimators are penalized in following formula:

$$\hat{\beta} = (X^T X + \lambda I)^{-1} X^T y ,$$

where λ is the ridge parameter which controls the amount of bias induced into the model. The ridge parameter was optimised using leave-one-subject-out cross-validation. β-coefficients were

estimated over N-1 subjects and then the BOLD signal of remaining subject was predicted with estimated β-coefficients. Prediction error (PE) for the remaining subject was calculated as:

$$PE = \sqrt{\sum_{1}^{K} (y - \hat{\beta}\, X)^2},$$

where K is the number of voxels and y is the BOLD signal in the i:th voxel. Cross-validation was repeated for every subject and average prediction error over all subjects was used as a measure of the model's fit to the data. Automatic optimiser function (https://www.mathworks.com/help/matlab/ref/fminbnd.html) was used to optimise ridge parameter for minimum prediction error and then β-coefficients for all subjects were estimated with optimised ridge parameter ($\lambda = 83$ for initial low-level regression and $\lambda = 28$ for the following social + low-level model). Prior to statistical modelling the BOLD signals were divided by their mean to make the regression coefficients more comparable between different individuals (Chen et al., 2017). A flowchart of ridge regression optimisation process is shown in **Figure SI-6**.

Comparison of low-level and social models

In addition of controlling low-level features in the analyses for social dimensions we also compared the predictions of separate low-level and social models as supplementary analysis. First, we run separate Ridge regression analyses with the low-level model (11 predictors) and with the social model (13 predictors), where no low-level features were controlled. Then, we compared the predictions of the models by calculating predictive R^2-values for each subject in the leave-one-subject-out cross validation process and then averaging the voxelwise predictive R^2-values over all subjects. Because the models had unequal number of predictors, we used adjusted R^2 for the model comparison. In the results we report where in the brain the social model gave more accurate predictions than the low-level model in terms of predictive adjusted R^2 (FDR-corrected, $q=0.05$). We also run the classification analysis only in these voxels to assess the classification accuracy of these regions compared to the whole brain or anatomical ROI classification accuracies.

Supplementary Results

Comparison of low-level and social models

Separate Ridge regression analyses for BOLD signal were conducted for both low-level and social models. In terms of predictive adjusted R^2, the social model predicted the BOLD signal significantly better in many cortical areas including voxels from functional areas STS, LOTC, TPJ and anatomical areas FG, SPG, IFG and precentral gyrus (**Figure SI-10**). Low-level model including audiovisual properties and the mean signals from CSF and WM predicted the BOLD response significantly better in most brain regions including primary visual and auditory areas. Classification analysis using only voxels with significantly higher predictive adjusted R^2 compared to low-level model yielded in 35% ($p<0.01$) total classification accuracy which is comparable with the highest observed classification accuracy in anatomical ROIs (34% in lingual gyrus).

Supplementary figures

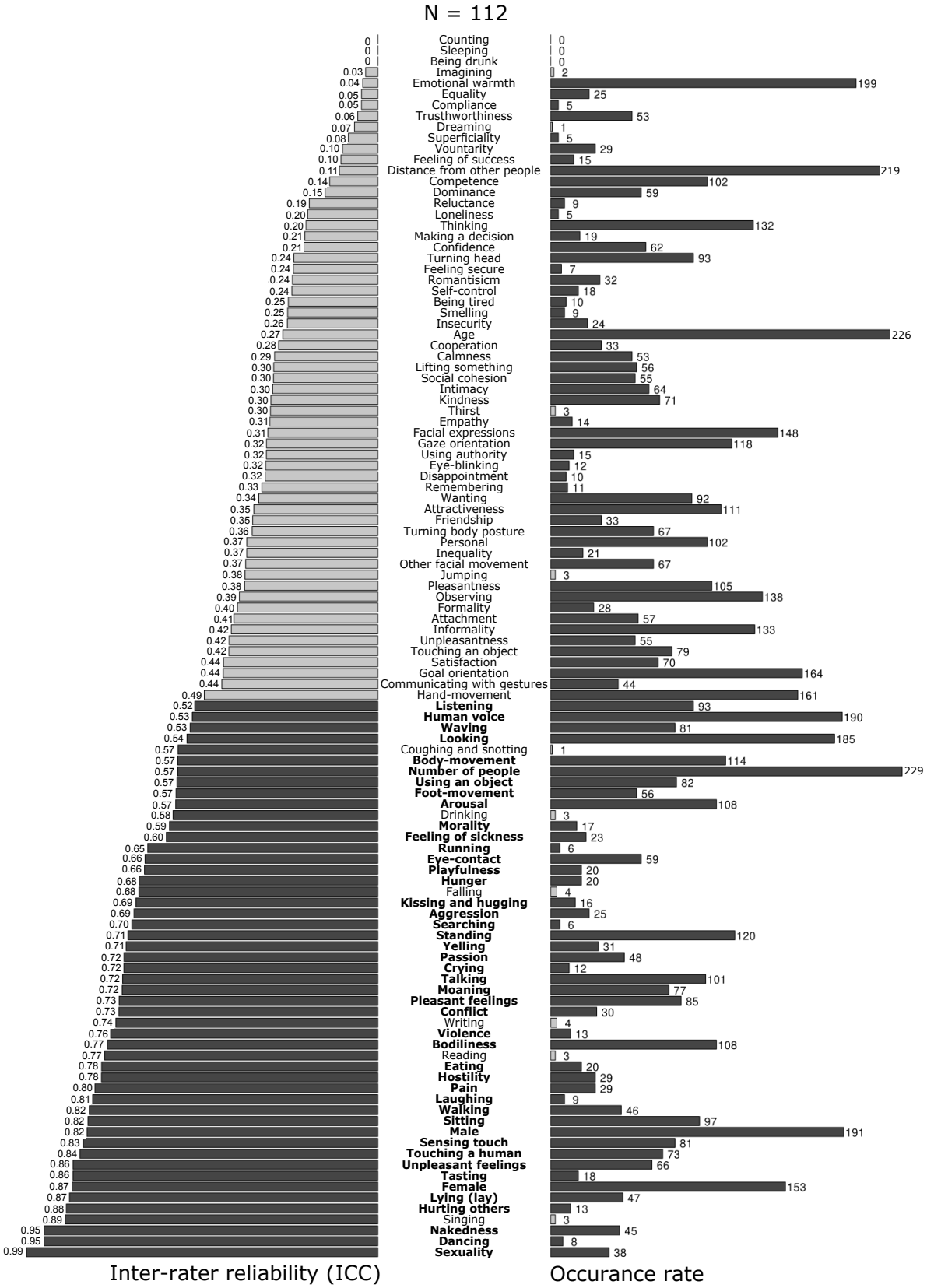

Supplementary Figure 1. *Inter-rater reliability and occurrence rate for all 112 features. Selected features (N=45) are bolded.*

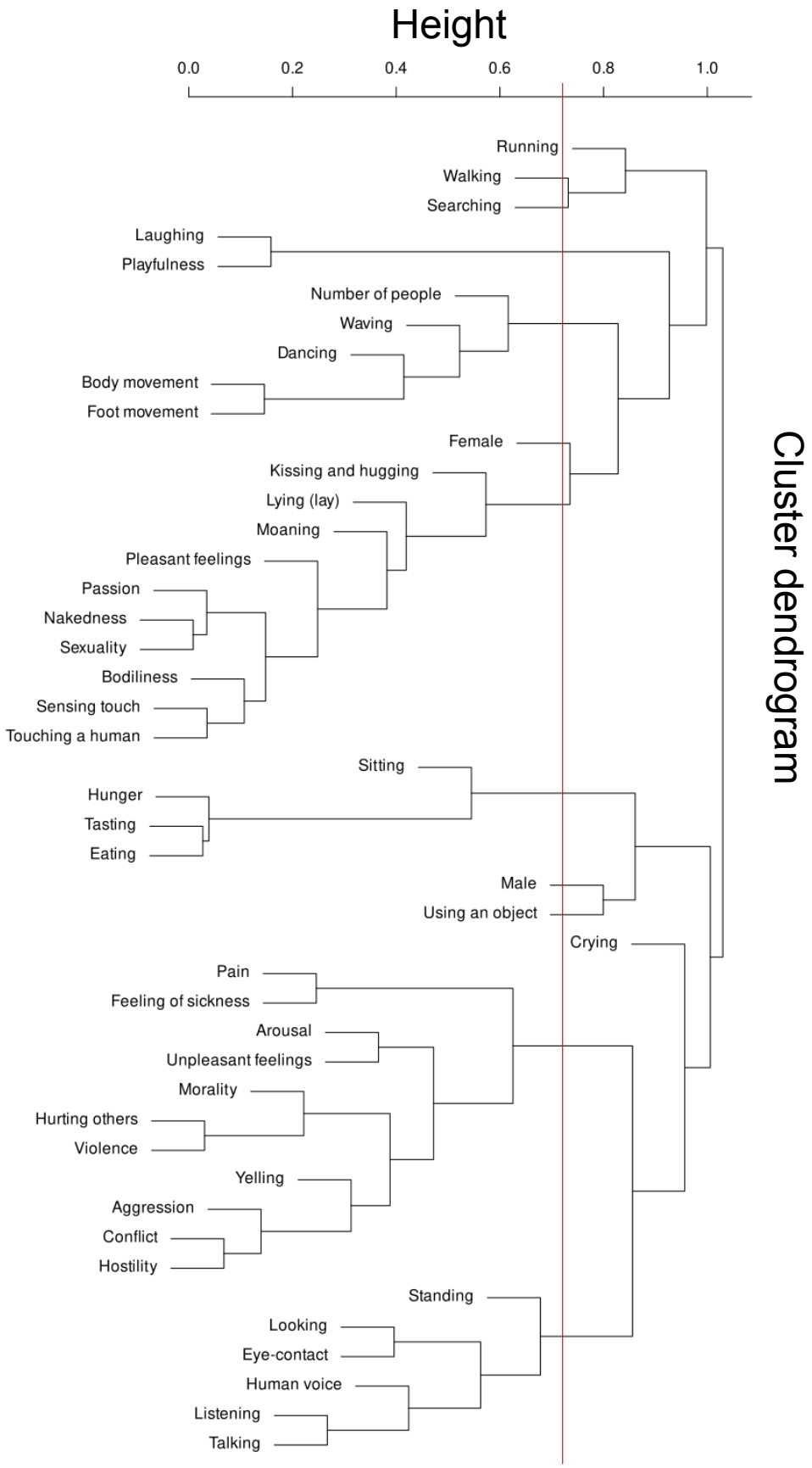

Supplementary Figure 2. *Hierarchical dendrogram of selected features and a vertical line indicating height of cluster boundaries.*

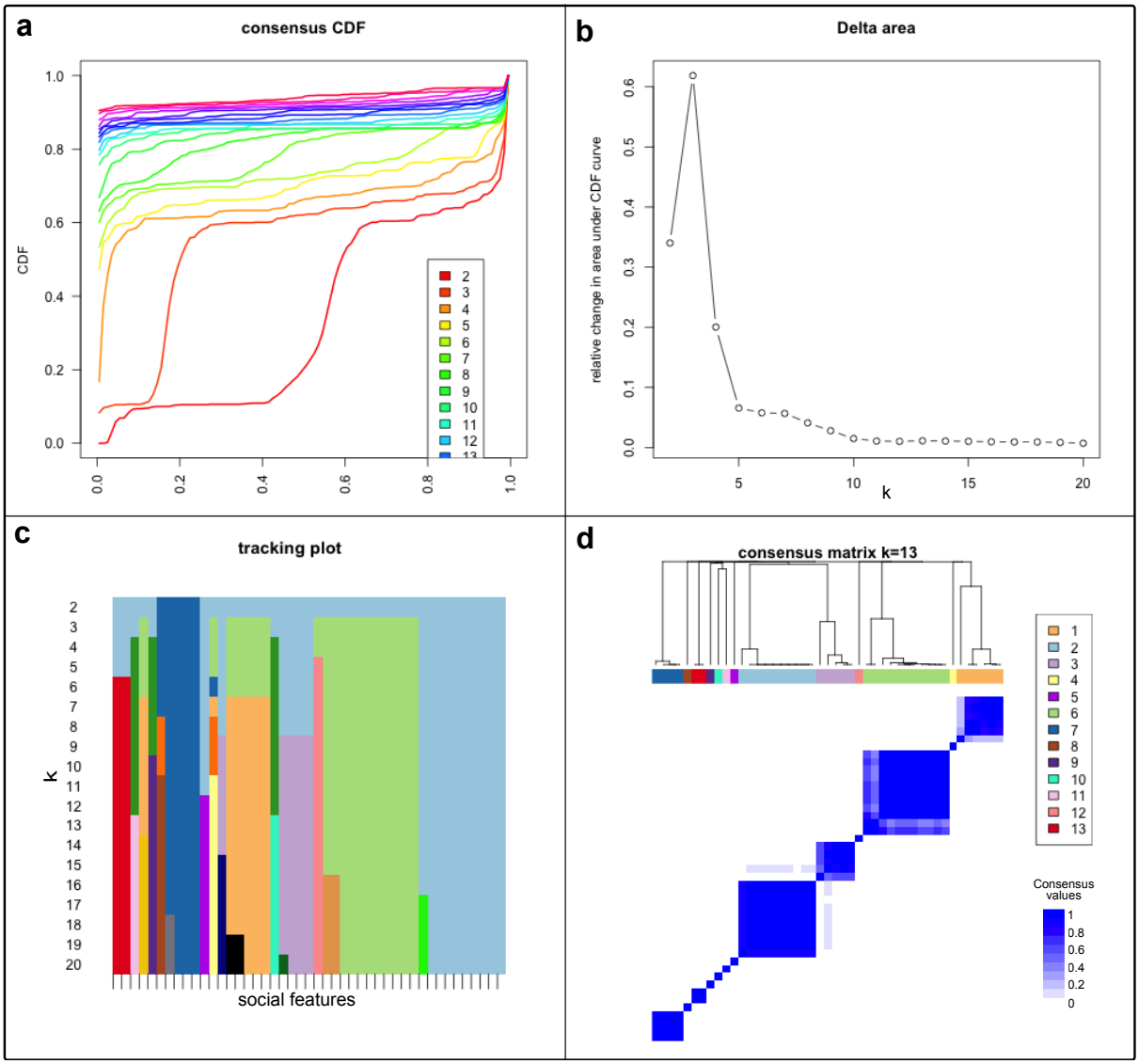

Supplementary Figure 3. *Results of the consensus clustering analysis with UPGMA as the clustering algorithm. a) Cumulative distribution function (CDF) of the consensus matrix for different number (k) of clusters. b) Relative change in area under curve between CDF of k clusters and k-1 clusters. c) Tracking plot showing changes in cluster structures with different number of clusters. d) Heatmap of the consensus values (1=always clustered together, 0=never clustered together) between social features (k=13).*

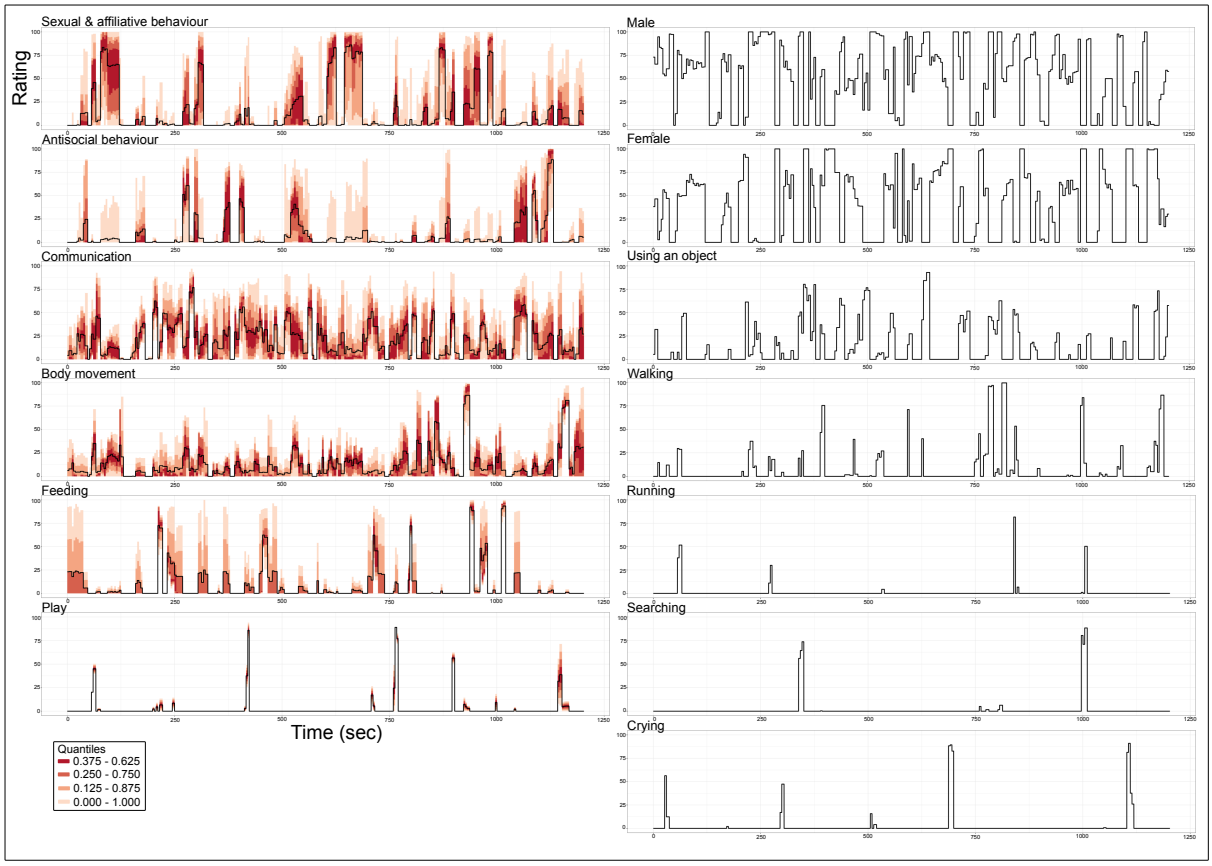

Supplementary Figure 4. *Rating time series for each social dimension. The time series for cluster dimensions (on the left) show the mean rating over all social features within the cluster, while social features included as separate social dimensions are plotted independently (on the right).*

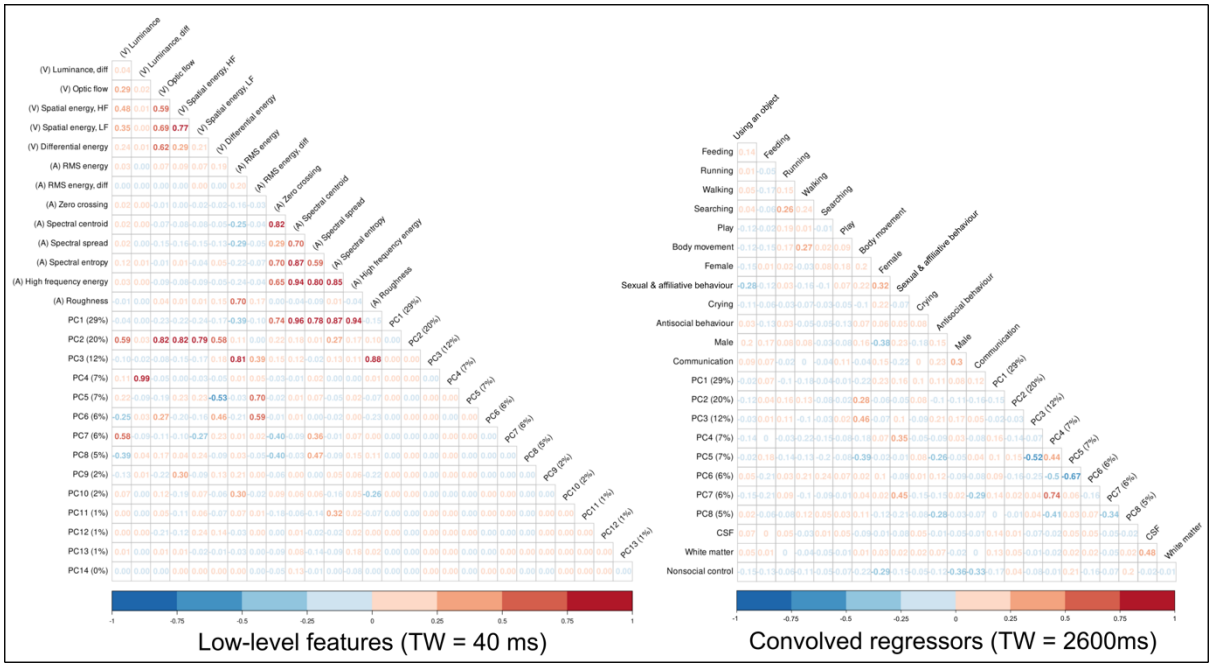

Supplementary Figure 5. *Correlations between low-level audiovisual features and main social dimensions. The left panel shows the extracted low-level audiovisual features and their correlations with corresponding principal components (PCs) in unconvolved form. The right panel shows the correlation between convolved regressors.*

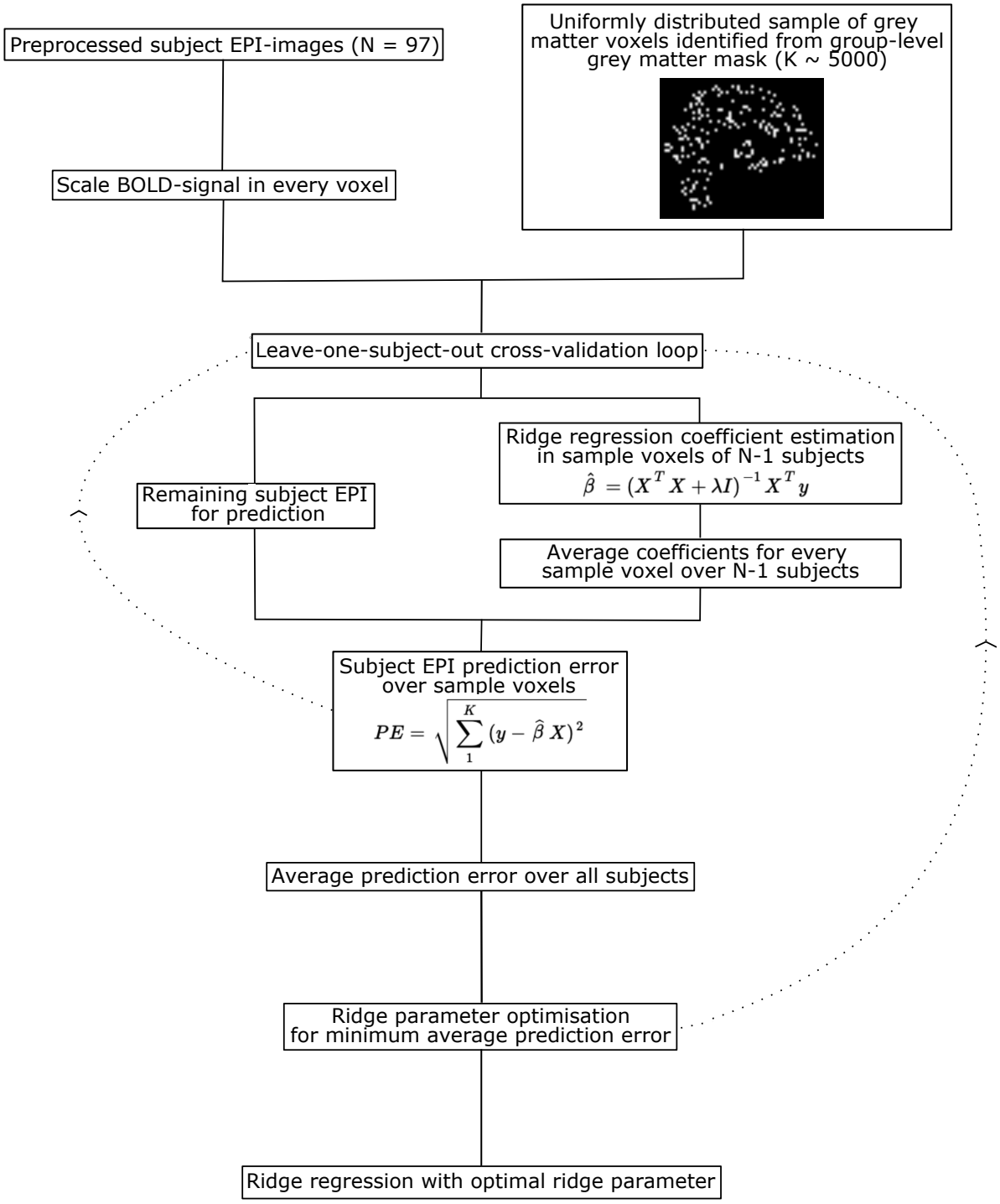

Supplementary Figure 6. *Ridge regression optimisation process. Ridge regression parameter (λ) was optimised using leave-one-subject-out cross-validation.*

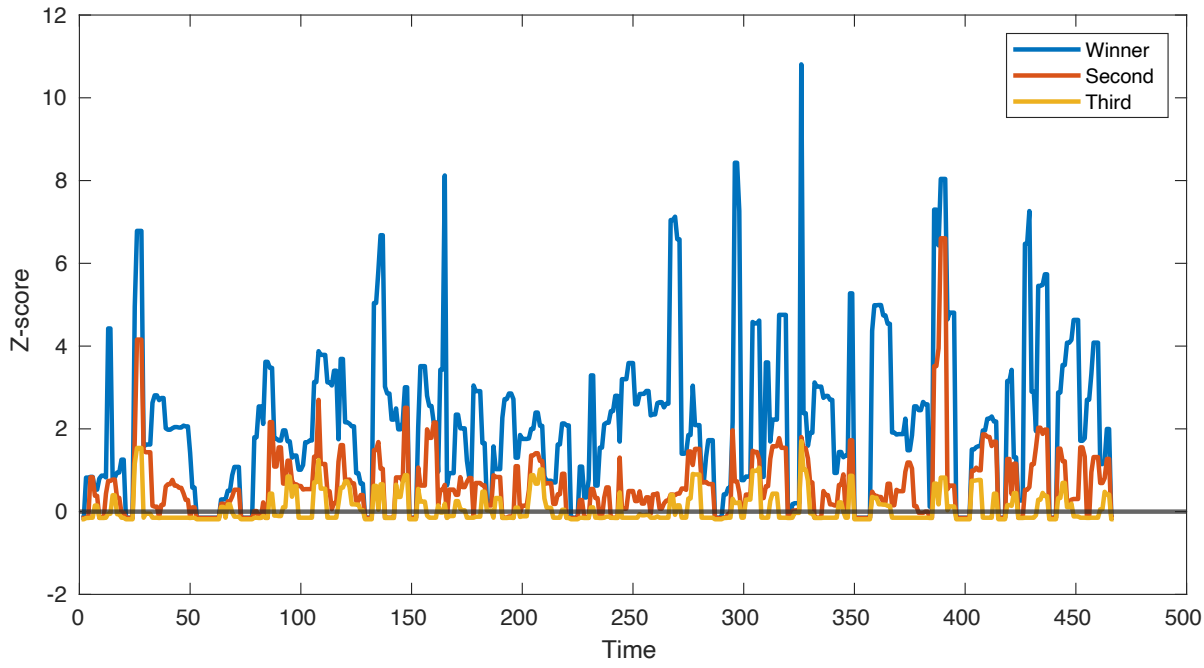

Supplementary Figure 7. *Z-scores of the highest, the 2nd highest and the 3rd highest Z-scores of social dimensions for each fMRI time point. The social label for each time point before classification was chosen from the dimension with the highest Z-score. No label was given to the time points where even the highest Z-score was below zero (horizontal line).*

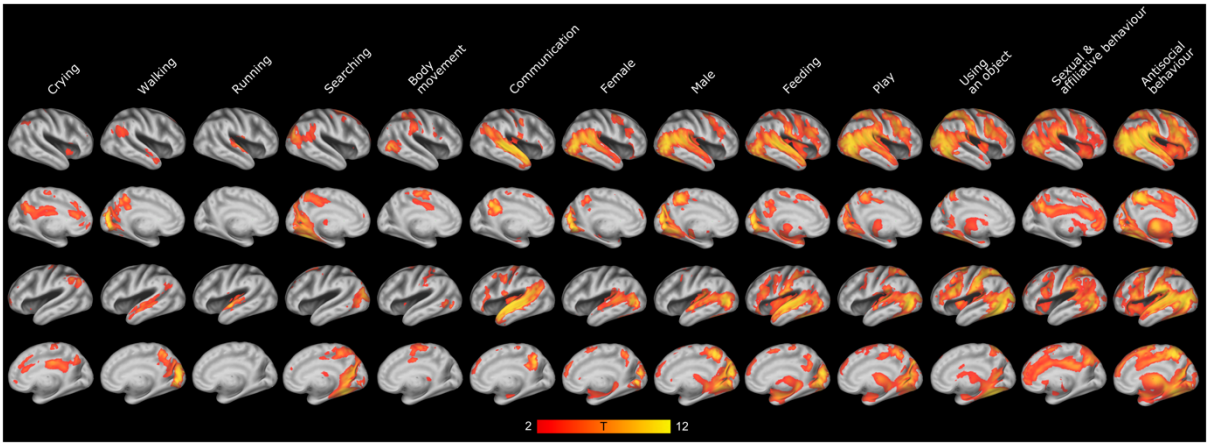

Supplementary Figure 8. *Brain regions showing increased BOLD activity for the social dimensions. Results show the voxelwise T-values (FDR-corrected, q = 0.05) of increased BOLD activity for each social dimension from the multiple regression analysis. See also Figure 3.*

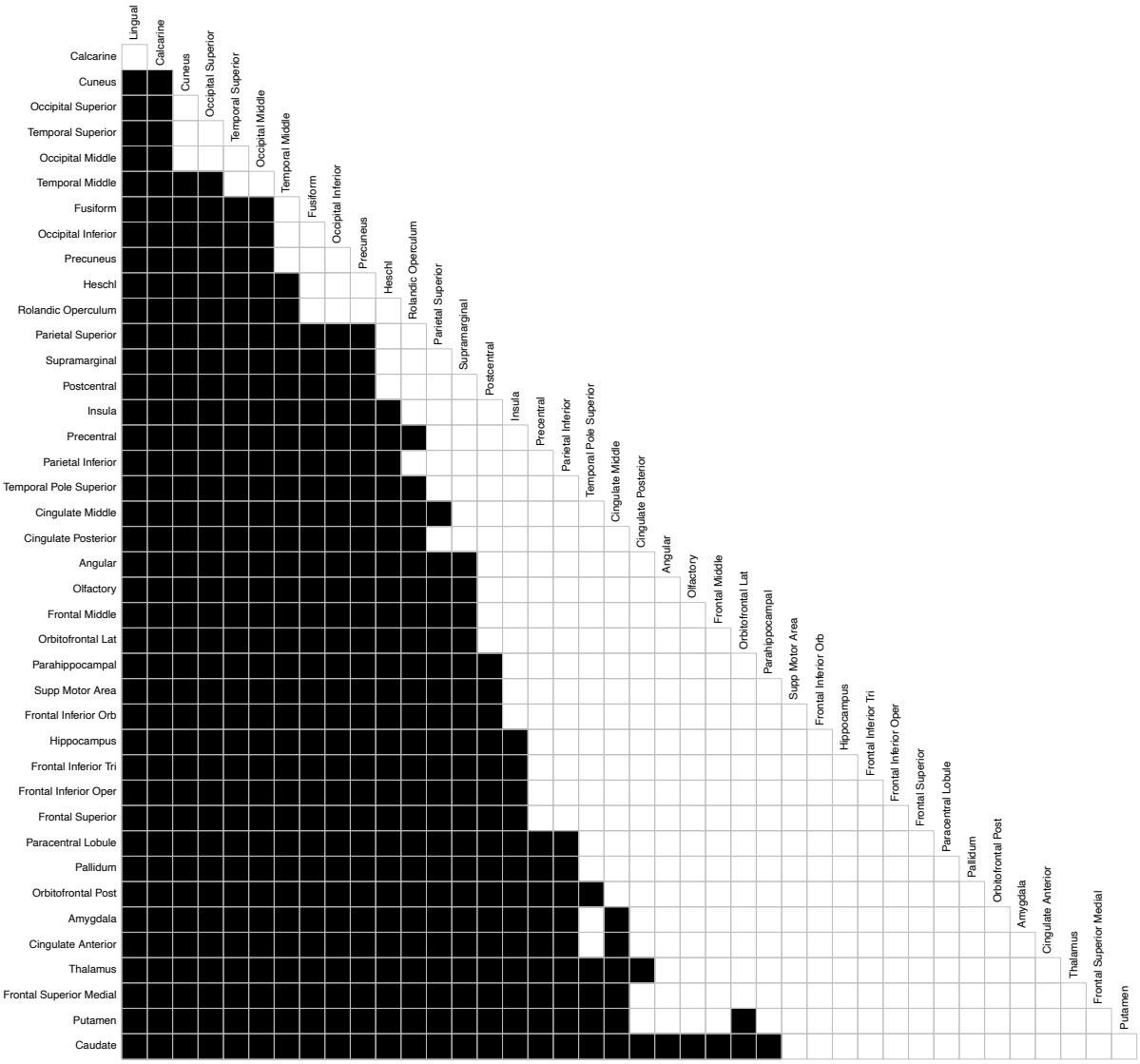

Supplementary Figure 9. *Comparison of* ROIs *in classification accuracies for social dimensions. Significant ($p<0.05$, Bonferroni corrected, paired t-test) differences between* ROIs *are marked black and* ROIs *are ordered from the highest classification accuracy (Lingual) to the lowest (Caudate) similarly as in figure 5. Black rectangle states that the* ROI *in the column has significantly higher classification accuracy than the* ROI *in the corresponding row. Figure 5 visualizes the gradient in classification accuracies of social dimensions and this figure confirms the observed gradient statistically.*

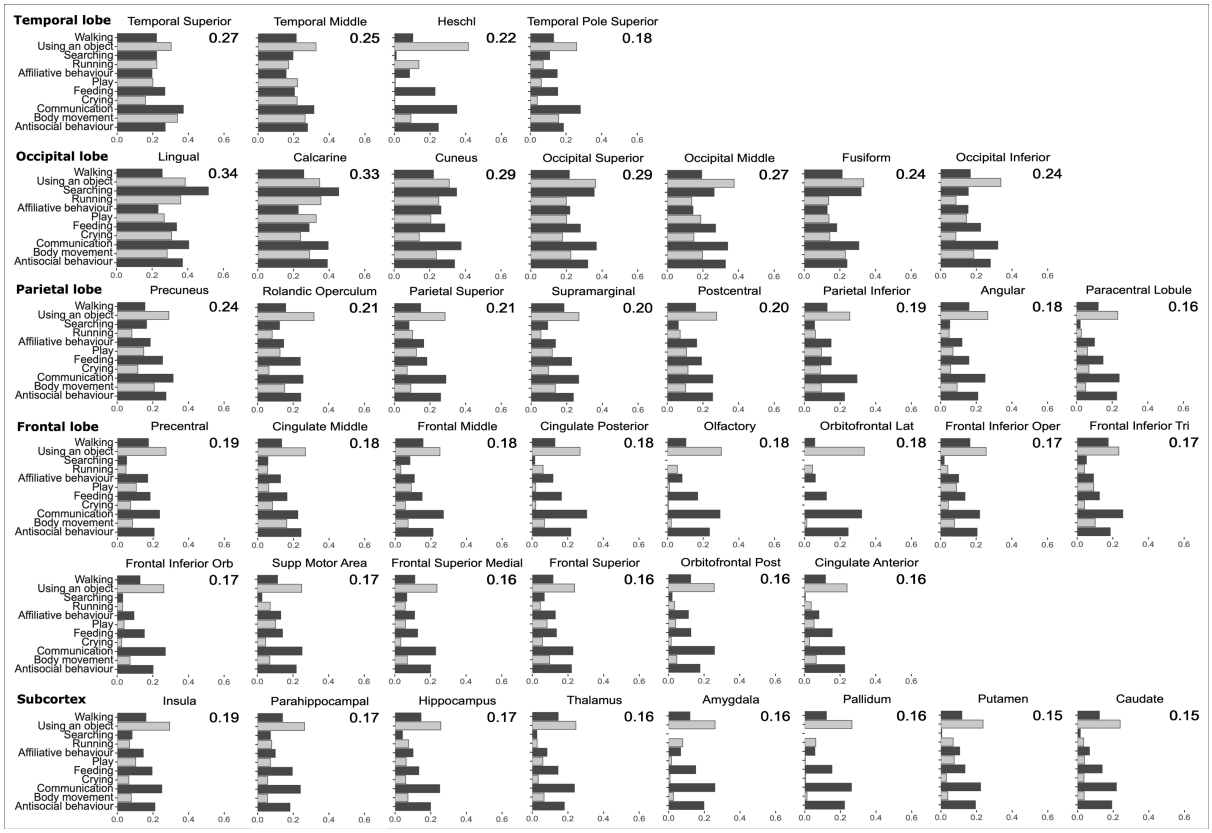

Supplementary Figure 10. *Region-of-interest classification results for perceptual social dimensions. Regional differences in the prediction accuracies to individual classes cannot be addressed.*

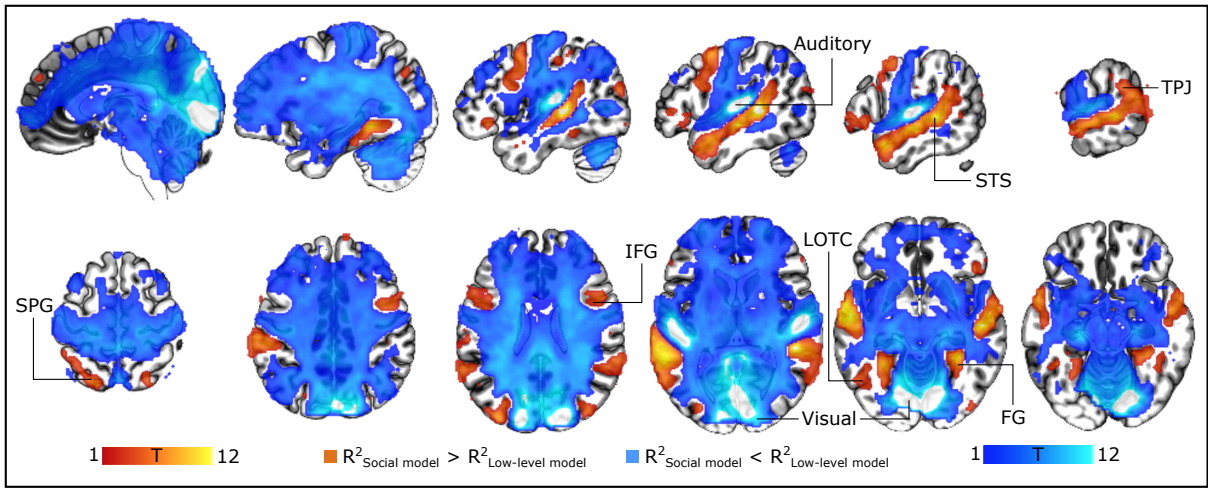

Supplementary Figure 11. *Comparison of social and low-level models. Statistically significant (FDR corrected, q = 0.05) differences in predictive adjusted* R^2 *values between social and low-level models from multivariate regression analysis.*

Supplementary tables

Supplementary Table 1. *Short descriptions of the contents of the 96 movie clips used as stimulus. See separate .xlsx file for the Table-SI1.*

All annotated socioemotional features, N = 112

Sensory input	Basic body functions	Person characteristics	Inner states	Social interaction signals	Social interaction characteristics
Smelling	Hand-movement	Age	Thinking	Communicating with gestures	Friendship
Pain	Turning head	Distance form other people	Dreaming	Singing	Equality
Looking	Turning body posture	Pleasantness	Feeling uncertain	Dancing	Inequality
Tasting	Jumping	Unpleasantness	Confidence	Talking	Attachment
Sensing touch	Falling	Attractiveness	Empathy	Listening	Intimacy
	Lifting something	Kindness	Self-control	Laughing	Romanticism
	Facial expressions	Trustworthiness	Emotional warmth	Crying	Formality
	Other facial movement	Competence	Remembering	Yelling	Informality
	Eye-blinking	Dominance	Feeling of success	Moaning	Personal
	Gaze orientation	Nakedness	Feeling secure	Kissing and hugging	Superficiality
	Coughing and snotting	Male	Thirst	Eye-contact	Compliance
	Touching an object	Female	Being tired	Touching a human	Using authority
	Sleeping		Disappointment	Hurting others	Voluntarity
	Drinking		Imagining		Cooperation
	Counting		Wanting		Reluctance
	Reading		Being drunk		Violence
	Writing		Calmness		Morality
	Body-movement		Making a desicion		Conflict
	Foot-movement		Observing		Number of people
	Running		Satisfaction		Human voice
	Walking		Social cohesion		Sexuality
	Lying (lay)		Loneliness		Bodiliness
	Standing		Goal orientation		Playfulness
	Waving		Pleasant feelings		Hostility
	Sitting		Unpleasant feelings		Aggression
	Using an object		Hunger		
	Searching		Passion		
	Eating		Arousal		
			Feeling of sickness		

Data-driven clusters of selected socioemotional features, N = 13

Sexual & affiliative behaviour	Antisocial behaviour	Communication	Body-movement	Feeding	Play	Individual features
Kissing and Hugging	Pain	Talking	Body-movement	Hunger	Laughing	Male
Pleasant feelings	Aggression	Listening	Foot-movement	Eating	Playfulness	Female
Passion	Conflict	Human voice	Dancing	Tasting		Walking
Sexuality	Hostility	Eye-contact	Waving	Sitting		Running
Nakedness	Feeling of sickness	Looking	Number of people			Searching
Bodiliness	Morality	Standing				Crying
Sensing touch	Hurting others					Using an object
Touching a human	Violence					
Moaning	Unpleasant feelings					
Lying (lay)	Yelling					
	Arousal					

Supplementary Table 2*. Complete listing of annotated socioemotional features (N=112). Features with insufficient inter-rater reliability or occurrence rate are marked with red color. Data-driven clusters (perceptual dimensions) of selected features (N = 13) are shown in the bottom section.*

Total accuracy	Minimum accuracy (class)	Minimum precision (class)	SEM of total prediction accuracy	Param: hidden_layers	Param: nodes	Param: alpha	Param: max_iter	Runtime (min)
0,482	0,415	0,424	0,0087	1	100	0,0001	500	73
0,473	0,404	0,416	0,0090	1	100	0,0001	1000	61
0,475	0,377	0,435	0,0086	1	100	0,1000	500	57
0,471	0,388	0,430	0,0086	1	100	0,1000	1000	58
0,486	0,409	0,442	0,0089	1	100	1,0000	500	57
0,483	0,410	0,437	0,0089	1	100	1,0000	1000	57
0,483	0,399	0,429	0,0083	1	200	0,0001	500	77
0,492	0,412	0,436	0,0087	1	200	0,0001	1000	78
0,486	0,399	0,423	0,0090	1	200	0,1000	500	75
0,488	0,410	0,414	0,0084	1	200	0,1000	1000	75
0,485	0,404	0,432	0,0088	1	200	1,0000	500	79
0,492	0,404	0,430	0,0085	1	200	1,0000	1000	78
0,501	0,436	0,450	0,0102	2	100	0,0001	500	58
0,502	0,407	0,453	0,0095	2	100	0,0001	1000	57
0,503	0,423	0,457	0,0089	2	100	0,1000	500	57
0,507	0,436	0,446	0,0095	2	100	0,1000	1000	58
0,519	**0,451**	**0,476**	**0,0098**	**2**	**100**	**1,0000**	**500**	**59**
0,519	0,454	0,460	0,0104	2	100	1,0000	1000	59
0,522	0,437	0,456	0,0094	2	200	0,0001	500	81
0,528	0,474	0,483	0,0095	2	200	0,0001	1000	81
0,528	0,445	0,469	0,0091	2	200	0,1000	500	76
0,524	0,432	0,473	0,0097	2	200	0,1000	1000	77
0,537	0,445	0,503	0,0099	2	200	1,0000	500	91
0,534	0,472	0,484	0,0101	2	200	1,0000	1000	91

Supplementary Table 3. *Results of neural network classifier parameter tuning. The whole brain classification was performed with a set of different parameter values for the classifier algorithm. Optimal parameters (hidden layers = 2, nodes = 100, alpha = 1.0, maximum iteration = 500) for the final analysis was chosen based on the algorithm's prediction accuracies, precisions, and algorithm runtime.*

Anatomical	
Cingulate Ant	Anterior cingulate cortex
Cingulate Post	Posterior cingulate cortex
FG	Fusiform gyrus
IFG	Inferior frontal gyrus
IFG Oper	Opercular part of inferior frontal gyrus
IFG Orb	Orbital part of inferior frontal gyrus
IFG Tri	Triangular part of frontal inferior gyrus
IOccG	Inferior occipital gyrus
IPG	Inferior parietal gyrus
MidFG	Middle frontal gyrus
MOccG	Middle occipital gyrus
MTG	Middle temporal gyrus
OFC Lat	Lateral orbitofrontal cortex
OFC Post	Posterior orbitofrontal cortex
Olfactory	Olfactory bulb
Rolandic Oper	Rolandic operculum
SFG	Superior frontal gyrus
SFG Med	Medial superior frontal gyrus
SOccG	Superior occipital gyrus
SPG	Superior parietal gyrus
STG	Superior temporal gyrus
SupM	Supramarginal gyrus
Supp Motor Area	Supplementary motor area
T Pole Sup	Superior temporal pole
Functional	
aSTS	Anterior superior temporal sulcus
Auditory	Primary auditory cortex
LOTC	Lateral occipitotemporal cortex
MFC	Medial frontal cortex
pSTS	Posterior superior temporal sulcus
STS	Superior temporal sulcus
TPJ	Temporoparietal junction
Visual	Primary visual cortex

Supplementary Table 4. *Table of abbreviations used in this article. Anatomical abbreviations refer to AAL2 atlas-based regions-of-interest. Functional regions-of-interest are used when interpreting the results in comparison with previous literature.*

References

Chen, G., Taylor, P. A., & Cox, R. W. (2017, 2017/02/15/). Is the statistic value all we should care about in neuroimaging? *Neuroimage, 147*, 952-959. https://doi.org/https://doi.org/10.1016/j.neuroimage.2016.09.066

Wilkerson, M. D., & Hayes, D. N. (2010, Jun 15). ConsensusClusterPlus: a class discovery tool with confidence assessments and item tracking. *Bioinformatics, 26*(12), 1572-1573. https://doi.org/10.1093/bioinformatics/btq170